

## **Supplementary Discussion**

### **1. Importance of asymmetric reconstruction**

In this study, all 3D reconstructions were determined and refined without imposing symmetry. In contrast, all previous negative-staining or cryo-EM studies of NSF and 20S supercomplex imposed either C3 or C6 point group symmetry, obscuring asymmetric features<sup>23–25</sup>. As a test, we reconstructed ADP-bound NSF and 20S supercomplex (state I) by imposing C6 and C3 symmetry, respectively. The resulting averaged map showed interpretable density for the D2 ring, but density features for the D1 and N domains do not match well with atomic models of these domains; for example, the N domains do not have the characteristic kidney shape observed in the crystal structure (Extended Data Fig. 5). More generally, this situation may be applicable to other previous cryo-EM studies of AAA+ ATPases, since asymmetry may have been present but overlooked by imposing presumed symmetry or by the inability to resolve asymmetric states in the refinement.

### **2. Comparison of NSF to other AAA+ family members**

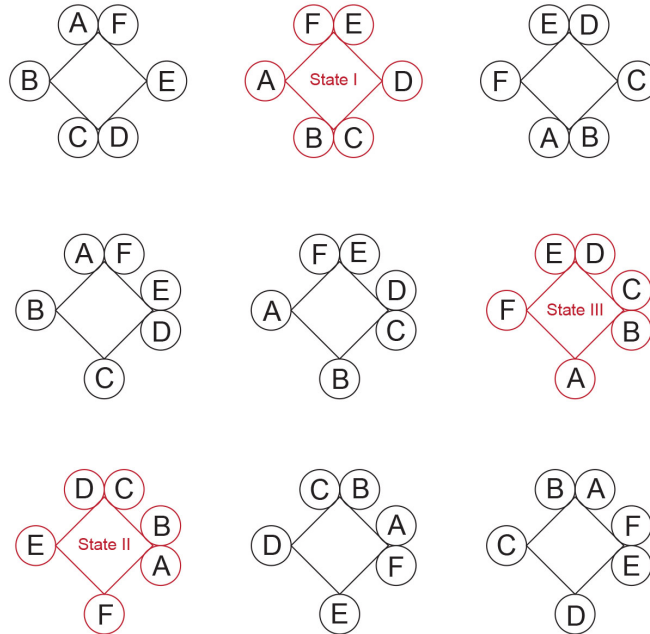
We determined structures of NSF in both ATP- and ADP-bound states using single particle cryo-EM to 4.2 and 7.6 Å, respectively. NSF is a homomeric hexamer consisting of two AAA+ ATPase rings. There are large conformational differences between ATP- and ADP-bound NSF in all three domains, especially for the D1 and N domains. The structure of the closest related enzyme VCP/p97 is symmetric in crystal structures<sup>28–30</sup>. Other closely related AAA+ members consisting of double ATPase rings do not show such asymmetric features, either<sup>67–69</sup>. However, a well-studied example

showing asymmetric arrangements is the prokaryotic translocase ClpX, a homomeric hexamer consisting of a single AAA+ ATPase ring<sup>70</sup>. A split-washer-like ATPase ring has been observed for papillomavirus E1 helicase, which binds to single stranded DNA<sup>71</sup>. Similar arrangement was also observed for EM studies of the 19S regulatory particle in the 26S proteasome, which is a heterohexameric AAA+ ATPase ring consisting of Rpt1-6 (ref. 72), as well as eukaryotic MCM helicases<sup>73,74</sup>. In terms of crystal structures, perhaps the most structurally similar example to the ATP-bound D1 ring of NSF is the transcriptional activator NtrC1, consisting of a single ATPase (AAA+) ring that also exhibits split-washer-like asymmetry. In addition, one of the domains behaves like Chain F of the D1 ring in NSF, stepping down towards the lower edge of the washer (Extended Data Fig. 6a)<sup>75</sup>. Interestingly, in very different biological contexts, large conformational changes and asymmetric ATPase rings have been observed for the RecA-like ATPase family<sup>76</sup>, which is related to, but not part of, the AAA+ family. We show in this study that the large-scale asymmetric transformation between ATP- and ADP-bound NSF likely plays a key role in NSF-mediated SNARE complex disassembly.

### **3. Nine theoretical patterns of N domain/ $\alpha$ SNAP interactions in the 20S supercomplex**

If one assumes that at most two N domains can interact with one SNAP and all four SNAPs interact with at least one N domain, there will be two possible configurations for six N domains to interact with four SNAPs: the dyad N domains are either in an opposite position or in a neighboring position. Since the D1 ring is not symmetric, each of the two configurations will result in six different patterns depending on the orientation

of the D1 ring (see the graph below). This leads to  $2 \times 6 = 12$  patterns. However, the patterns generated by opposite N domain dyads are redundant by a factor of 2. Thus, there are  $6 + 6/2 = 9$  unique patterns, as shown in the following diagram.



#### 4. A pore translocation mechanism is unlikely

It is possible that NSF also interacts with the SNARE complex through the pore loops of the D1 domain since the N termini of the SNARE complex are always located close to Chains E and F, which are at the raised edge of the D1 split washer (Figs. 4b and 7d). Such pore loops exist in AAA+ translocases, and can interact with substrate-peptides nonspecifically<sup>77</sup>. Although our 20S structures do not resolve possible interactions between the pore loops and SNARE complex, a “translocation” mechanism is unlikely since the D2 domains do not contain such pore loops. Rather, the pore loops are more likely to act as anchor points when applying a torque or shear force to the SNARE complex.

## **5. SNAP species and stoichiometry**

Although we used the most ubiquitous isoform of SNAP in higher eukaryotes,  $\alpha$ SNAP, exclusively in this study, our conclusions should be applicable to other SNAPs as well since their surface charges are highly conserved across different species and isoforms<sup>17,18,43</sup>. Different stoichiometry of the SNAP-SNARE subcomplex have been reported in the literature<sup>24,40,42,78,79</sup>, consistent with the promiscuous  $\alpha$ SNAP stoichiometry that we have observed.

## References

67. Guo, F., Maurizi, M. R., Esser, L. & Xia, D. Crystal structure of ClpA, an Hsp100 chaperone and regulator of ClpAP protease. *J. Biol. Chem.* **277**, 46743–52 (2002).
68. Wang, F. *et al.* Structure and mechanism of the hexameric MecA-ClpC molecular machine. *Nature* **471**, 331–5 (2011).
69. Lee, S. *et al.* The structure of ClpB: a molecular chaperone that rescues proteins from an aggregated state. *Cell* **115**, 229–40 (2003).
70. Glynn, S. E., Martin, A., Nager, A. R., Baker, T. A. & Sauer, R. T. Structures of asymmetric ClpX hexamers reveal nucleotide-dependent motions in a AAA+ protein-unfolding machine. *Cell* **139**, 744–56 (2009).
71. Enemark, E. J. & Joshua-Tor, L. Mechanism of DNA translocation in a replicative hexameric helicase. *Nature* **442**, 270–5 (2006).
72. Matyskiela, M. E., Lander, G. C. & Martin, A. Conformational switching of the 26S proteasome enables substrate degradation. *Nat. Struct. Mol. Biol.* **20**, 781–8 (2013).
73. Costa, A. *et al.* The structural basis for MCM2-7 helicase activation by GINS and Cdc45. *Nat. Struct. Mol. Biol.* **18**, 471–7 (2011).
74. Lyubimov, A. Y., Costa, A., Bleichert, F., Botchan, M. R. & Berger, J. M. ATP-dependent conformational dynamics underlie the functional asymmetry of the replicative helicase from a minimalist eukaryote. *Proc. Natl. Acad. Sci. U. S. A.* **109**, 11999–2004 (2012).
75. Sysoeva, T. A., Chowdhury, S., Guo, L. & Nixon, B. T. Nucleotide-induced asymmetry within ATPase activator ring drives  $\sigma$ 54-RNAP interaction and ATP hydrolysis. *Genes Dev.* **27**, 2500–11 (2013).
76. O'Shea, V. L. & Berger, J. M. Loading strategies of ring-shaped nucleic acid translocases and helicases. *Curr. Opin. Struct. Biol.* **25**, 16–24 (2014).
77. Sauer, R. T. & Baker, T. A. AAA+ proteases: ATP-fueled machines of protein destruction. *Annu. Rev. Biochem.* **80**, 587–612 (2011).
78. Wimmer, C. *et al.* Molecular mass, stoichiometry, and assembly of 20 S particles. *J. Biol. Chem.* **276**, 29091–7 (2001).
79. Shah, N., Colbert, K. N., Enos, M. D., Herschlag, D. & Weis, W. I. Three  $\alpha$ SNAP and 10 ATP Molecules Are Used In SNARE Complex Disassembly by N-

ethylmaleimide Sensitive Factor (NSF). *J. Biol. Chem.* (2014).  
doi:10.1074/jbc.M114.620849